

PHOTOCATALYTIC ACTIVITY OF Sr-DOPED LaCoO_3 UNDER UV ILLUMINATION

Do Van Phuong¹, Truong Le Bich Tram², Le Minh Vien¹

¹*Ho Chi Minh city University of Technology, VNU; lmvien@hcmut.edu.vn*

²*The University of Danang*

Abstract - The substituted perovskite photocatalysts $\text{La}_{1-x}\text{Sr}_x\text{CoO}_3$ ($x = 0, 0.2, 0.4, 0.6, 0.8$) were successfully prepared by sol-gel method. Some characterization techniques, such as XRD, SEM, TEM, UV-vis diffuse reflection spectroscopy, and Brumauer – Emmett – Teller (BET) were used to verify the structure and physico-chemical properties of catalysts. In addition, the effect of $\text{La}_{1-x}\text{Sr}_x\text{CoO}_3$ powders on the photocatalytic degradation of methylene blue and CO_2 reduction reaction under UV light source was also investigated. The results showed a maximum photocatalytic degradation of methylene blue 30 ppm could be achieved with a degradation degree of 11.32% by $\text{La}_{0.6}\text{Sr}_{0.4}\text{CoO}_3$ synthesized at 850°C for 4h (LSC64-850) in UV light for 150 min. Moreover, the photocatalytic results of CO_2 reduction reaction indicated that LSC64-850 catalyst had the methane yield of 12.27 $\mu\text{mol/g cat}$. Which was higher than that of undoped LaCoO_3 , 1.78 $\mu\text{mol/g cat}$.

Key words - Perovskite; photocatalyst; sol-gel method; degradation; CO_2 reduction reaction; methylene blue; methane

1. Introduction

Pollutant causing by dying substances has been warned as a serious problem over the world for many years [1]. Besides, the global warming issue is one of the major environmental concerns because of the rising demand for energy which significantly contribute to the increasing of CO_2 greenhouse gas emissions [2]. Based on the report of Fujishima and Honda about the photocatalytic splitting of water into hydrogen and oxygen using TiO_2 in 1972 [3], environmental photocatalysis has become a promising and sustainable approach in solving the above problems.

In the past decades, numerous valuable and cheap photocatalysts were investigated, such as TiO_2 [4], ZnO [5], Fe_2O_3 [6], CdS [7]. However, these photocatalysts have a limitation in use that they can only absorb the ultra-violet light because of their wide band gap. In recent years, various new materials have been successfully fabricated. Among of them, perovskite-type oxides (ABO_3 ; A = a rare earth cation and B = a transition metal cation) have attracted considerable attentions due to their unique properties such as various types of oxygen vacancy order, intrinsic oxygen reduction reaction activity, high conductivity and magnetic properties [8]. A number of typical perovskite oxides have been demonstrated as candidate material for photocatalysis, such as SrTiO_3 [9], LaCoO_3 [10], LaFeO_3 [11] and $\text{Ba}_{0.5}\text{Sr}_{0.5}\text{Co}_{0.8}\text{Fe}_{0.2}\text{O}_3$ [12]. Among perovskite-type, lanthanum cobaltate, LaCoO_3 , was cheap, environmentally friendly and highly active in oxidation processes, making it a strong promising material for many applications including catalytic reduction of NO_x in automotive exhausts, CO_2 reduction reaction, catalytic oxidation of volatile organic compounds (VOCs) and photocatalytic degradation reactions [8]. Further research indicated that the photocatalysis of perovskite-base materials can be enhanced by doping. For example, $\text{La}_{0.6}\text{Sr}_{0.4}\text{CoO}_3$ photocatalyst exhibited much higher

photocatalytic activity in the 2-propanol degradation than that of pure LaCoO_3 [13]. Moreover, Ming Meng (2012) [14] reported that among all the catalysts that fabricated by the simultaneous replacement for La^{3+} and Co^{2+} by K^+ and Ni^{3+} , the $\text{La}_{0.9}\text{K}_{0.1}\text{Co}_{0.95}\text{Ni}_{0.05}\text{O}_3$ has the highest performance in NO_x removal. In addition, $\text{La}_{0.7}\text{Ba}_{0.3}\text{CoO}_3$ showed optimal photocatalytic activity with a degradation degree of malachite green up to 97% compared to 70.1% of pure LaCoO_3 [1].

In this research, perovskite $\text{La}_{1-x}\text{Sr}_x\text{CoO}_3$ ($x = 0, 0.2, 0.4, 0.6, 0.8$) photocatalysts were synthesized by sol-gel method and characterized with several techniques such as XRD, SEM and UV-DRS to clearly understand the effect of Sr-doping. Finally, the methylene degradation and CO_2 reduction reaction was carried out to evaluate the photocatalytic activity of $\text{La}_{1-x}\text{Sr}_x\text{CoO}_3$ powders.

2. Experimental

2.1. Materials

$\text{La}(\text{NO}_3)_3 \cdot 6\text{H}_2\text{O}$, $\text{Sr}(\text{NO}_3)_2$, $\text{Co}(\text{NO}_3)_2 \cdot 6\text{H}_2\text{O}$, citric acid monohydrate ($\text{C}_6\text{H}_8\text{O}_7 \cdot \text{H}_2\text{O}$) and methylene blue were obtained from Sigma Aldrich. All the chemicals used in the experiments were of reagent grade and were used without further purification.

2.2. Synthesis of $\text{La}_{1-x}\text{Sr}_x\text{CoO}_3$

The flowchart of the experimental process was shown in Figure 1. A series of perovskite photocatalysts $\text{La}_{1-x}\text{Sr}_x\text{CoO}_3$ with variable Sr content ($x = 0, 0.2, 0.4, 0.6, 0.8$) were fabricated by the sol-gel citrate method. The metal nitrates were weighed to the nominal compositions and dissolved in 60 mL deionized water with Co concentration of 0.25 mol/L. Citric acid monohydrate, $\text{CA} \cdot \text{H}_2\text{O}$, was also added to this solution as chelating agent with molar ratio of citric acid/metals to be 1.5/1. The resulting mixture was then heated in water bath at 70°C under continuous stirring. After 4h heating, the clear pink solution transformed into gel. This dark pink gel was dried in an oven in air at 140°C overnight and following calcined at 850°C for 4h with heating rate of 5 °C/min. In order to obtained perovskite powders as photocatalytic materials, the 850 °C calcined powders were pulverized in ethanol media using 5mm dia. zirconia balls in 12h and following drying in electric oven in overnight. The obtained perovskite powders were labeled as LSC followed by two numbers where the first two indicate the molar ratio between lanthanum and strontium, and the last three numbers indicates the calcined temperature. For instance, the $\text{La}_{0.6}\text{Sr}_{0.4}\text{CoO}_3$ sample prepared at 850°C was labeled as LSC64-850. However, when x is equal to 0, the product was marked simply as LC-850.

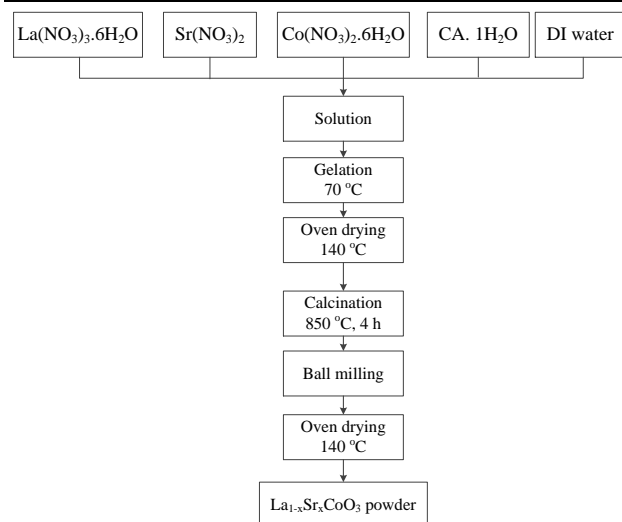


Figure 1. Flowchart of $\text{La}_{1-x}\text{Sr}_x\text{CoO}_3$ synthesis process by sol-gel method

2.3. Characterization

X-ray diffraction (XRD) patterns of the specimens were recorded using an X-ray diffractometer (D2 Phaser, Bruker) equipped with a $\text{Cu K}\alpha$ radiation source (1.5406 \AA) and nickel filter. Microstructure analysis was performed with a scanning electron microscope (SEM, JSM-6500F, JEOL). Ultraviolet-visible (UV-vis) diffuse reflection spectroscopy of the photocatalyst was investigated with a spectrometer (Varian Cary-100) UV-vis spectrophotometer in the wavelength between 200 nm and 800 nm using BaSO_4 as a reference. In addition, specific surface area of LSC64-850 powder was measured by the Brumauer – Emmett – Teller (BET) method using (Quantochrome NOVA 1000e, Nitrogen).

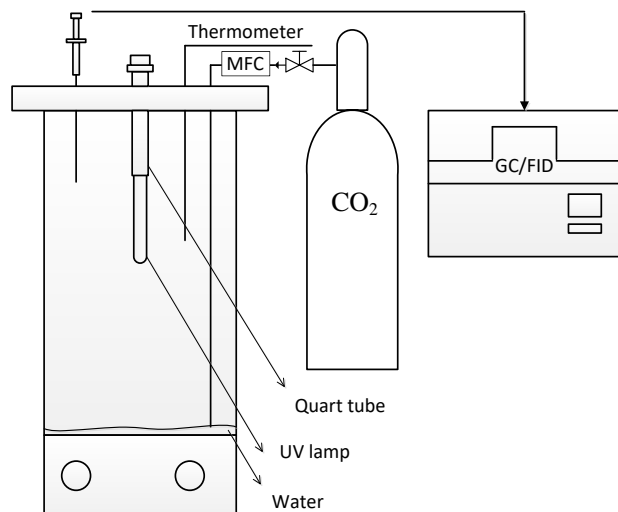


Figure 2. Experimental setup model for the photocatalytic reduction of CO_2

2.4. Photocatalytic degradation of methylene blue experiment

In order to evaluate influence of Sr content on MB photodegradation, the suspensions containing methylene blue and $\text{La}_{1-x}\text{Sr}_x\text{CoO}_3$ photocatalyst were irradiated by the Pen-Ray® Light Source lamp with continuous magnetic stirring at room temperature. The 0.5 g/L suspension was

prepared by adding 0.5 g nano perovskite $\text{La}_{1-x}\text{Sr}_x\text{CoO}_3$ into 1.0 L of 30ppm MB solution. Prior to UV irradiation, the suspensions were magnetically stirred for 65 min in the dark to ensure adsorption/desorption equilibrium of methylene blue with the catalyst. After that, the mixture was subjected to UV irradiation. 6 ml of the supernatant was taken out by syringe at different time intervals and centrifuged to separate the catalyst and MB solution. The MB concentration remaining after photocatalytic treatment was determined using 4001/4 UV-visible spectrophotometer with wavelength of 664 nm.

2.5. Photocatalytic reduction of CO_2 experiment

The experimental setup for the photocatalytic reduction of CO_2 was shown in Figure 2. In the liquid phase reaction, the catalyst loading was 0.1g of LC-850 or LSC64-850 in 5.0 ml distilled water. Before each test, the solution was saturated with CO_2 by flowing CO_2 gas (99.999%) for 30 min. The experiments were then carried out in a batch reactor with the temperature controlled at 60°C and UV-irradiated using a 9W UV lamp with wave length of 254 nm. The main product of CO_2 reduction reaction, CH_4 , was analyzed by a gas chromatography (China Chromatography 9800) equipped with a flame ionization detector (FID).

A blank test was carried out similar to CO_2 reduction experiment but without photocatalysts present.

3. Results and discussion

3.1. Characterization of photocatalysts

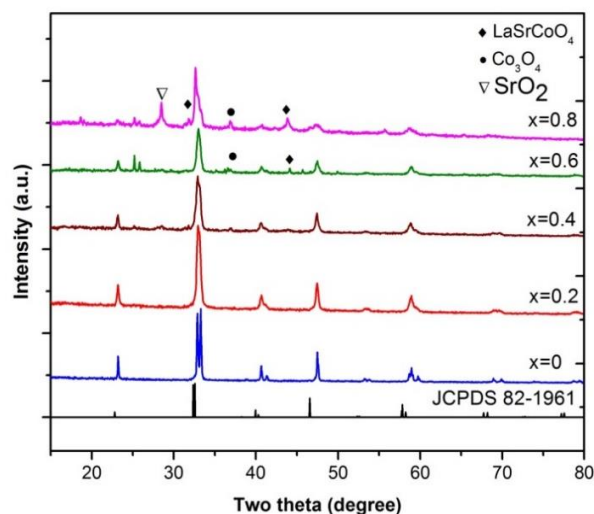


Figure 3. XRD patterns of $\text{La}_{1-x}\text{Sr}_x\text{CoO}_3$ ($x = 0, 0.2, 0.4, 0.6$ and 0.8) powders

The XRD pattern of $\text{La}_{1-x}\text{Sr}_x\text{CoO}_3$ powders are shown in Figure 3. Results showed that XRD patterns of $\text{La}_{1-x}\text{Sr}_x\text{CoO}_3$ ($x = 0, 0.2, 0.4$) are well-indexed to perovskite structure of LaCoO_3 (JCPDS 82-1961). Minor strange diffraction peaks appeared in the XRD patterns of the LSC28-850 and LSC46-850 powders indicated unexpected impurities phases of LaSrCoO_4 [13], Co_3O_4 [13] and SrO_2 [10]. The intensities of these strange peaks increased with increasing Sr content from $x = 0.6$ to $x = 0.8$. The presence of such impurities, detected only for

the large quantities of strontium ($x = 0.6, 0.8$), can be ascribed to the different ionic radius La^{3+} 1.032 Å [13], Sr^{2+} 1.18 Å [13] that affects the crystal strain and symmetry.

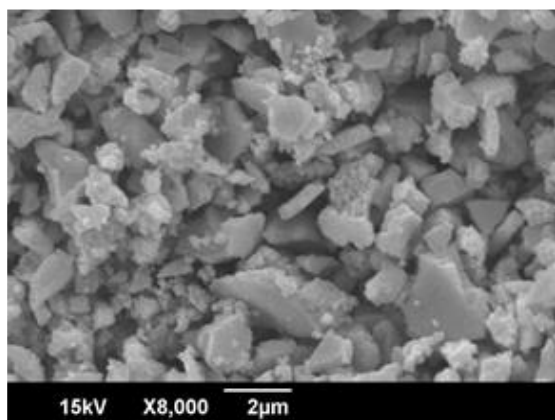


Figure 4. SEM image of $\text{La}_{0.6}\text{Sr}_{0.4}\text{CoO}_3$ powder

Fig. 4 is the SEM image of LSC64-850 powder, with sharp edges and corners particles. As seen from the image, the particles are not uniform and have large sizes ranging from 1 µm – 2 µm. The large particle size lead to low specific surface value of 10.94 m²/g.

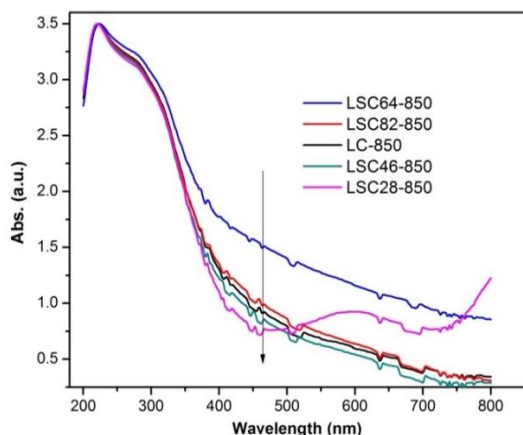


Figure 5. UV-vis diffuse absorption spectra of $\text{La}_{1-x}\text{Sr}_x\text{CoO}_3$ powders

Fig. 5 showed the UV-vis absorption spectra obtained by diffuse reflection of $\text{La}_{1-x}\text{Sr}_x\text{CoO}_3$ ($x = 0, 0.2, 0.4, 0.6, 0.8$). The absorption band spectra were used for the determination of the band gap using the equation of $E_g = 1240/\lambda$ [2]. As can be seen from the Fig. 5, the band gap of LaCoO_3 was 2.8 eV according to the optical absorption thresholds at 443 nm. The band gap of $\text{La}_{1-x}\text{Sr}_x\text{CoO}_3$ ($x = 0.2, 0.4, 0.6, 0.8$) were 2.75 eV, 2.72 eV, 2.86 eV and 2.92 eV according to the optical absorption thresholds at 450 nm, 456 nm, 433 nm and 425 nm, respectively. Band gap of catalysts decreased with increasing of the amount of Sr substitution from $x = 0$ to $x = 0.4$. However, it started to increase with increasing Sr-substituted level due to suppressing lanthanum cobalt oxide quality with additional impurity phase as shown in Figure 3.

3.2. Photocatalytic degradation of methylene blue

The degradation of aqueous methylene blue solution (MB) was performed under UV light to explore the

photocatalytic activity of the $\text{La}_{1-x}\text{Sr}_x\text{CoO}_3$ samples. The results were showed in Fig. 6. The degradation efficiency of methylene blue increased with increasing irradiation time, and then reached equilibrium after 85 min photocatalytic reaction. After 85 min of irradiation, the degradation of MB by $\text{La}_{1-x}\text{Sr}_x\text{CoO}_3$ ($x = 0, 0.2, 0.4, 0.6, 0.8$) reached 5.45%, 7.86%, 11.32%, 8.68%, 9.51%, respectively. The result indicated that all Sr-doped samples exhibited photocatalytic activities slight higher than that of undoped LaCoO_3 . The photocatalytic degradation performance increased with the increasing Sr doping level, x equals 0 to 0.4; however, the degradation efficiency decreased when the Sr doping level was over 0.4. In other words, $\text{La}_{0.6}\text{Sr}_{0.4}\text{CoO}_3$ exhibited the best photocatalytic activity in MB degradation due to smallest band gap possession.

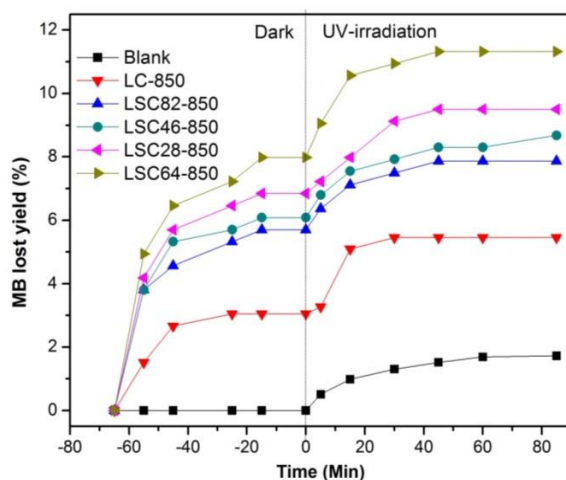


Figure 6. Photocatalytic activity of MB degradation with $\text{La}_{1-x}\text{Sr}_x\text{CoO}_3$ ($x = 0, 0.2, 0.4, 0.6, 0.8$) catalysts under UV light

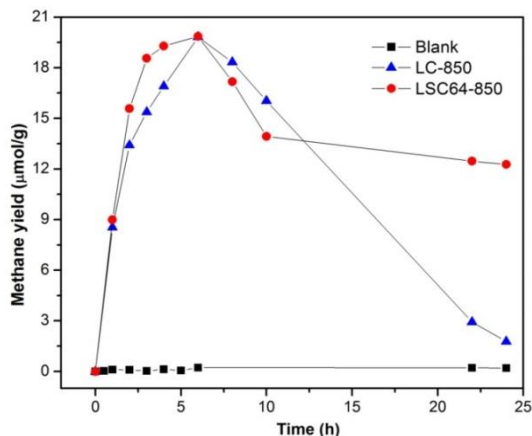


Figure 7. Photocatalytic reduction of CO_2 with LC-850 and LSC64-850 photocatalysts under UV light

3.3. Photocatalytic reduction of CO_2

Figure. 7 showed the photocatalytic activity of LSC64-850 and LC-850 powders for the CO_2 reduction reaction. After 24h of UV illumination, the methane production rate by using LSC64-850 photocatalyst was measured 12.27 µmol/g of cat., much higher than that of LC-850 to be 1.78 µmol/g cat. This may be because LSC64-850 catalyst possesses smaller band gap and more oxygen vacancies [1, 14] due to acceptor doping. However,

the CH₄ yield was suppressed after 6 hours irradiation. This implied that CH₄ is able to convert into other compound, resulting in a decrease of CH₄ yield.

4. Conclusion

In this study, La_{1-x}Sr_xCoO₃ photocatalysts were successfully synthesized using sol-gel method with x values from 0 to 0.4. However, In particular, LSC64-850 material had the smallest band gap with specific surface area of approximately 10.94 m²/g. We also investigated the photocatalytic activity of Sr-doped LaCoO₃ catalysts for the methylene blue degradation and CO₂ reduction reaction under UV light. The results indicated that LSC64-850 powder exhibited the highest MB degradation efficiency with degradation degree of 11.32% under UV light for 150min. Moreover, LSC64-850 photocatalyst could achieve a methane production rate of 12.27 μmol/g of cat under UV light. However, the MB degradation and CO₂ reduction experiments conducted in this study were at UV light (365 nm and 254 nm, respectively); this is a limitation of this research. Therefore, the further experiments should be performed in the visible light to expand the application of perovskite-type La_{1-x}Sr_xCoO₃ photocatalyst and these process.

Acknowledgements

The authors would like to acknowledge the support of Prof. Wu, Department of Chemical Engineering, National Taiwan University for using CO₂ reduction photoreactor as well as his valued contribution.

REFERENCES

- [1] Chunqiu Zhang, Hongcai He, Ning Wang, Haijun Chen, Deting Kong, *Visible-light sensitive La_{1-x}Ba_xCoO₃ photocatalyst for malachite green degradation*, Ceramics International 39, pp. 3685 – 3689, 2013.
- [2] Hung-Yu Wu, Hsunling Bai and Jeffrey C. S. Wu, *Photocatalytic reduction of CO₂ using Ti-MCM-41 photocatalysts in monoethanolamine solution for methane production*, Ind. Eng. Chem. Res 53, pp. 11221-11227, 2014.
- [3] A. Fujishima, K. Honda, *Electrochemical photolysis of water at a semiconductor electrode*, Nature 238, pp. 37-38, 1972.
- [4] M.-C. Wang, H.-J. Lin, C.-H. Wang, H.-C. Wu, *Effects of annealing temperature on the photocatalytic activity of N-doped TiO₂ thin films*, Ceramics International 38, pp. 195-200, 2012.
- [5] S. Suwanboon, P. Amornpitoksuk, N. Muensit, *Dependence of photocatalytic activity on the structural and optical properties of nanocrystalline ZnO powders*, Ceramics International 37, pp. 2247-2253, 2011.
- [6] Michael R. Hoffmann, Scot T. Martin, Wonyong, Choi, Detlef W. Bahnemann, *Environmental applications of semiconductor photocatalysis*, Chem. Rev. 95 (1), pp. 69-96, 1995.
- [7] Qizhao Wang, Jiajia Li, Yan Bai, Juhong Lian, Haohao Huang, Zhimin Li, Ziqiang Lei, Wenfeng Shangguan, *Photochemical preparation of Cd/CdS photocatalysts and their efficient photocatalytic hydrogen production under visible light irradiation*, Green Chem. 16, pp. 2728, 2014.
- [8] Shasha Fu, Helin Niu, Zhiyin Tao, Jiming Song, Changjie Mao, Shengyi Zhang, Changle Chen, Dong Wang, *Low temperature synthesis and photocatalytic property of perovskite-type LaCoO₃ hollow spheres*, Journal of Alloys and Compounds 576, pp. 5-12, 2013.
- [9] Yang Liu, Lei Xie, Yan Li, Rong Yang, Jianglan Qu, Yaoqi Li, Xingguo Li, *Synthesis and high photocatalytic hydrogen production of SrTiO₃ nanoparticles from water splitting under UV irradiation*, Journal of Power Sources 183, pp. 701-707, 2008.
- [10] Bahman Seyfi, Morteza Baghalha, Hossein Kazemian, *Modified LaCoO₃ nano-perovskite catalysts for the environmental application of automotive CO oxidation*, Chemical Engineering Journal 148, pp. 306-311, 2009.
- [11] Peisong Tang, Yi Tong, Haifeng Cheng, Feng Cao, Guoxiang Pan, *Microwave-assisted synthesis of nanoparticulate perovskite LaFeO₃ as a high active visible-light photocatalyst*, Current Applied Physics 13, pp. 340-343, 2013.
- [12] Jin Suntivich, Kevin J. May, Hubert A. Gasteiger, John B. Goodenough, Yang Shao-Horn, *A perovskite oxide optimized for oxygen evolution catalysis from molecular orbital principles*, Science 334, 1383, 2011.
- [13] E. García – López, G. Marci, F. Puleo, V. La Parola, L.F. Liotta, La_{1-x}Sr_xCo_{1-y}Fe_yO_{3-δ} perovskites: *Preparation, characterization and solar photocatalytic activity*, Applied Catalysis B: Environmental, 2014.
- [14] Zhaoqiang Li, Ming Meng, Fangfang Dai, Tiandou Hu, Yaning Xie, Jing Zhang, *Performance of K and Ni substituted La_{1-x}K_xCo_{1-y}Fe_yO_{3-δ} perovskite catalysts used for soot combustion, NO_x storage and simultaneous NO_x-soot removal*, Fuel 93, pp. 606-610, 2012.

(The Board of Editors received the paper on 05/06/2015, its review was completed on 05/22/2015)